

Complementarity of Gamma-ray and LHC Searches for Neutralino Dark Matter in the Focus Point Region

E. Moulin^{1,*}, A. Jacholkowska¹, G. Moutaka¹, J.-L. Kneur¹, E. Nuss¹,
T. Lari², G. Polesello³, D. Tovey⁴, M. White⁵, and Z. Yang⁶

¹ *Laboratoire de Physique Théorique et Astroparticules, CNRS/IN2P3 et Université Montpellier 2,
Place Eugène Bataillon, F-34095 Montpellier Cedex, France*

² *INFN, Sezione di Milano, Via Celoria 16, I-20133 Milano, Italy*

³ *INFN, Sezione di Pavia, Via Bassi 6, I-27100 Pavia, Italy*

⁴ *Department of Physics and Astronomy, University of Sheffield, Hounsfield Road, Sheffield S3 7RH, UK*

⁵ *Cavendish Laboratory, University of Cambridge,
Madingley Road, Cambridge, CB3 0HE, UK and*

⁶ *Department of Physics, Carleton University, Ottawa, ON K1S 5B6, Canada*

(Dated: October 29, 2018)

We study the complementarity between the indirect detection of dark matter with γ -rays in H.E.S.S. and the supersymmetry searches with ATLAS at the Large Hadron Collider in the Focus Point region within the mSUGRA framework. The sensitivity of the central telescope of the H.E.S.S. II experiment with an energy threshold of ~ 20 GeV is investigated. We show that the detection of γ -ray fluxes of $\mathcal{O}(10^{-12}) \text{ cm}^{-2} \text{ s}^{-1}$ with H.E.S.S. II covers a substantial part of the Focus Point region which may be more difficult for LHC experiments. Despite the presence of multi-TeV scalars, we show that LHC will be sensitive to a complementary part of this region through three body NLSP leptonic decays. This interesting complementarity between H.E.S.S. II and LHC searches is further highlighted in terms of the gluino mass and the two lightest neutralino mass difference.

PACS numbers: 95.35.+d, 11.30.Pb, 12.60.Jv, 95.55.Ka

Keywords: Dark Matter, Supersymmetry, SUGRA, Cherenkov telescopes, LHC physics, relic density

I. INTRODUCTION

A preferred particle physics candidate for the Dark Matter (DM) component in the Universe is an electrically neutral Lightest Supersymmetric Particle (LSP), which in various supersymmetry (SUSY) breaking scenarios is the lightest neutralino χ [1, 2]. The self-annihilations of neutralinos in halos of galaxies would produce Standard Model particles: γ , ν , charged leptons and hadrons. The ongoing and forthcoming ground-based (H.E.S.S. [3], MAGIC [4], VERITAS [5] and space (AMS [6], GLAST [7], PAMELA [8]) experiments detecting galactic cosmic rays will open large new windows for the DM annihilation signal detection. In particular, phase II of the H.E.S.S. experiment will provide an improved sensitivity due to a combination of a large effective area, low energy threshold, and an excellent angular resolution necessary for the efficient hadron background suppression.

Simultaneously to the new generation of the cosmic ray detectors which will provide outstanding data in the dark matter detection domain, the Large Hadron Collider (LHC) start-up in 2008 will explore physics in the TeV energy range and thus probe the origin of electroweak symmetry breaking. It will also introduce a new

era of physics and particle searches beyond the Standard Model, and in particular ought to discover the new particles predicted by supersymmetry or other new states such as those foreseen by models with extra spatial dimensions. Under the hypothesis that dark matter is composed of a SUSY (or Kaluza-Klein) particle, a relationship between the astrophysical signal observation and the properties of the new particles found at LHC can be established. The information from LHC measurements will also allow us to discard various hypotheses on the nature of the DM [9]. On the other hand, in case of a signal detection which is not correlated with an astrophysical source, H.E.S.S. would be able to investigate the DM distribution profile in halos of galaxies independently of the particle physics uncertainties. Accurate reconstruction of the morphology of the sources could help to discard specific halo models.

The aim of this paper is to study some experimental and phenomenological aspects of the complementarity between searches of SUSY particles in the ATLAS experiment and the detection potential of the H.E.S.S. telescope in phase II, in the case of the so-called Focus Point (FP) region in the mSUGRA framework of the Minimal Supersymmetric Model (MSSM). The most realistic Monte Carlo simulations for both experiments will provide input to this study. As the measured variables in ATLAS are related to various mass differences of the SUSY states, the H.E.S.S. II sensitivity will be investigated with respect to these variables. In particular, we will investigate the dependence of the gamma-ray fluxes and the annihilation cross-section on the gluino mass and

*Electronic address: emmanuel.moulin@cea.fr; Also at IRFU(ex-DAPNIA)/SPP, CEA Saclay, F-91191 Gif-sur-Yvette, Cedex, France

the mass difference of the two lightest neutralinos. Detailed studies in the literature have investigated the complementarity of accelerator measurements at LHC/ILC and astrophysical observations, e.g. [10, 11], to unveil the nature of Dark Matter. Here, we focus on the complementary constraints in the FP region with the forthcoming atmospheric Cherenkov telescope H.E.S.S. II and LHC searches using realistic performances for both experiments. This FP region is also of great interest for searches via neutrino telescopes [12].

The rest of the paper is organized as follows: some key points of the supersymmetric focus point framework and related phenomenological features are given in section 2. Section 3 describes various issues related to γ -ray signals expected in Cherenkov telescopes and the detection sensitivity of the upcoming phase II of the H.E.S.S. experiment. The constraints from the γ -ray flux sensitivity to the parameter space in the focus point region are studied in section 4. MSSM spectrum measurements at the LHC for this parameter space region are discussed in section 5. Section 6 is devoted to the potential complementarity between H.E.S.S. II and ATLAS measurements. Conclusions and perspectives are given in section 7.

II. SUPERSYMMETRIC FRAMEWORK AND THE FOCUS POINT REGION

We consider the framework where supersymmetry breaking in a hidden sector is mediated to the visible world through gravitational interactions between the very heavy hidden fields and the MSSM sector. Although little is known about the actual dynamics responsible for this breaking and its mediation mechanisms, it is reasonable to assume that the gross features of the low energy spectrum can be encapsulated in a universality assumption (and possible deviations from it) for the effective soft supersymmetry breaking parameters at a scale close to the Planck or the GUT scale. The more detailed features of this spectrum are then determined by quantum effects obtained through the running down to the electroweak scale. It is important to keep in mind that the theoretical uncertainties at the high (SUSY breaking) scale are different in nature from those involving the running to the low (electroweak) scale. The former cannot be reduced without a better knowledge of the underlying new physics, while the latter are in principle reducible through the improved calculational theoretical tools such as the Renormalization Group Evolution (RGE) codes and spectrum calculators, where for instance scale dependencies, threshold effects, higher order corrections, etc... are standardized. In practice, the effects of these two types of uncertainties are not easy to disentangle when one tries to determine in a model-independent bottom-up approach the fundamental parameters of the model, ultimately starting from experimental data. Moreover, in a collider environment such as the LHC one would presumably aim first at typical SUSY discovery events,

then at the determination of mass differences of various SUSY particles which are kinematically accessible. With this respect, resorting to detailed predictions in a top-down approach should be taken only as a guide for the possible patterns of SUSY mass spectra, production rates, branching ratios, etc..., as well as the complementary requirements for a good dark matter candidate (relic density, predictions for direct and indirect dark matter searches).

In this paper we focus on MSSM spectrum patterns where all the scalar quarks and leptons are in the multi-TeV range and thus out of direct reach at the LHC, while the lighter neutralinos and charginos and of course the lightest Higgs remain accessible. Such patterns are motivated by the so-called focus point scenarios [13] where it is noted within mSUGRA that for $\tan\beta \gtrsim 5$ and $m_{1/2}, A_0 \lesssim 1$ TeV, m_0 could be very large and still allow electroweak symmetry breaking and the right Z boson mass to occur without a large fine-tuning between the order parameter $m_{H_u}^2 (\leq 0)$ and $\mu^2 (\geq 0)$ at the electroweak scale. This feature is due to the quantum effects which push the running of $m_{H_u}^2$ to an essentially unique value, a focus point, at some given low scale, irrespective of its initial value at very high scales. It so happens that for the above range of parameters this focus point occurs at a scale Q_0 of order the electroweak scale, and where $|m_{H_u}(Q_0)|$ is also of the same order, together with $\mu^2(Q_0) (\sim m_{H_u}^2(Q_0))$ due to electroweak symmetry breaking (EWSB). In this case, the smallness of the μ parameter leading to a non negligible higgsino component for the lightest neutralino has immediate consequences on the dark matter issues [14, 15], reducing the neutralino relic density and increasing the reaction rates and fluxes respectively for direct and indirect dark matter detection. These distinctive features, together with other ones due to the heaviness of the sfermion sector (such as the suppression of flavor changing neutral currents and the electric dipole moments of the electron and the neutron) makes this scenario with low fine-tuning very interesting to study. However, the low fine-tuning in the EWSB condition seems to be traded for a very large sensitivity to the top yukawa coupling and thus to the physical top mass, as was shown in various studies in [16] (see also [15]). The practical consequence of this sensitivity is the important dispersion in the output of different spectrum calculator and RGE codes and thus in the predictions of the various experimental observables, not to mention numerical convergence issues as pointed out in [15] through a comparison of the two codes ISAJET 7.69 [17] and SUSPECT 2.34 [18]. These features hint at the need for further standardisation of the various codes through the inclusion of improved calculations at similar levels; but we anticipate that this would probably not be enough to improve substantially the situation, due to the intrinsic high sensitivity on input parameters in the focus point regions. For that, one would require a better theoretical understanding of this high sensitivity (meaning of the dependence of the focus

point location on the running scale, etc). Since in the present study we are mainly interested in the potential of the experimental complementarity between H.E.S.S. phase II and ATLAS for the challenging multi-TeV spectrum pattern, we will ignore the above theoretical uncertainties and consider the focus-point-like regions sticking for convenience to a given code, namely ISAJET [17] to generate the MSSM mass spectrum and couplings. We have however performed cross-checks with the SUSPECT code [18] and found reasonable agreement for the overall focus point region (see also section 4 for further discussions). The mSUGRA parameter space is defined by the following set of four parameters and a sign[58]:

$$m_0, m_{1/2}, A_0, \tan \beta, \text{sign}(\mu) \quad (1)$$

with m_0 the common scalar mass, $m_{1/2}$ the common gaugino mass, A_0 the trilinear coupling, $\text{sign}(\mu)$ the sign of the higgsino mass and $\tan \beta$ the Higgs vacuum expectation values (VEV) ratio. In the sequel of the paper, we will perform detailed scans of the parameter space in the focus point region using both ISAJET 7.69 interfaced with DarkSUSY 4.1 [19], and ISAJET 7.71.

III. INDIRECT DETECTION OF DARK MATTER

A. Galactic sources of dark matter halos

The choice of the astrophysical targets to be observed is of main importance for the dark matter signal searches. Among the most commonly suggested sources [20, 21, 22, 23], various studies such as [20] have shown that the Galactic Center could be an interesting object under the assumption that the DM density halo presents a strong density increase towards its inner region. The dark matter density profile extrapolated to the central region is currently parameterized following the cored spherical models as proposed by [24] or as halos with a cusp as proposed by [25] and [26]. The cuspieness of the halo is not yet confirmed by the rotation curves of the stars [27] and is in contradiction with a high value of the microlensing optical depth in the central region [28] which cannot be due to the diffuse DM but rather to the presence of faint stars and brown dwarfs. The other argument against the presence of a large density of the DM in the Galactic Center is its impact on the large galactic bar rotation which could be modified by the dynamical friction with dark matter medium [29]. However, microlensing optical depth and dynamical friction arguments are slightly controversial [30] and a cusp at the Galactic Center is not yet ruled out. It has to be underlined that the Galactic Center region is rich in potential γ -ray emitters such as supernova remnants, the supermassive black hole Sgr A*, the recently discovered HESS J1745-290 source [31], and the standard interactions of charged cosmic rays producing diffuse γ -ray emission [32].

The most promising astrophysical objects with large mass-to-luminosity ratio are the Spheroidal Dwarf Galaxies (dSph) of the Local Group, periodically crossing the Galactic Plane. The not too distant ones are Draco, Sagittarius and Canis Major located respectively at $\sim 80, 24$ and 8 kpc from the heliocentric position. The presently measured star rotation curves provide the mass-to-luminosity ratio in the range of 20 to 100 and no final answer has been given about cuspieness or not of the dark matter density profile, so the cored density profile should also be considered when predictions for γ -ray fluxes from the neutralino annihilations are performed. As the line-of-sight integration of dark matter density is mainly driven by the distance value of the object, the Canis Major galaxy is certainly the most promising target. On the other hand, this galaxy seems to be the most disrupted one by the tidal forces as it orbits our Milky Way. The expected flux ratios between dSphs and the Galactic Center taken as a reference source are respectively $\sim 0.03, 0.15$ and 0.5 for Draco, Sagittarius and Canis Major, as calculated for a Navarro-Frenk-White (NFW) cusped profile by [33]. Despite smaller γ -ray fluxes expected for dwarf galaxies, they consist of less complex environments compared to the Galactic Center region as pointed above and present lower background coming from astrophysical sources. The extended TeV emission along the galactic plane leads to a diffuse astrophysical background which is very challenging to overcome. Dwarf galaxies are currently in the scope of the H.E.S.S. experiment and first results on Sagittarius have been reported in [34].

In this paper we consider the Galactic Center as a benchmark source in order to compare our predictions with those provided by other authors. The γ -ray fluxes from annihilation of neutralinos in a spherical dark halo are obtained from

$$\frac{d\Phi_\gamma(\Delta\Omega, E_\gamma)}{dE_\gamma} = \frac{1}{4\pi} \frac{\langle\sigma v\rangle}{2m_\chi^2} \frac{dN_\gamma}{dE_\gamma} \times \bar{J}(\Delta\Omega) \Delta\Omega \quad (2)$$

with :

$$\bar{J}(\Delta\Omega) = \frac{1}{\Delta\Omega} \int_{\Delta\Omega} d\Omega \int_{l.o.s} \rho^2[r(s)] ds. \quad (3)$$

Eq. (2) is expressed as a product of a particle physics term and an astrophysics term. The former contains $\langle\sigma v\rangle$, the velocity-weighted annihilation cross-section, the neutralino mass m_χ and the gamma-ray annihilation spectrum dN_γ/dE_γ . The astrophysics part depends on ρ , the radial density profile expressed in terms of $r(s) = \sqrt{s^2 + s_0^2 - 2ss_0 \cos\theta}$ where s is the heliocentric distance of a given point along the line of sight (l.o.s) in the Galactic halo, s_0 is the heliocentric distance of the Galactic Center, and θ denotes the angle between the direction of the Galactic Center and the l.o.s. The integral over s ranges from 0 to $s_0 \cos\theta + \sqrt{R_0^2 - s_0^2 \sin^2\theta}$ where R_0 is the radial extension of the spherical halo. The integration is performed along the l.o.s. to the target and averaged over the solid angle $\Delta\Omega$ usually matching the angular resolution of the detector.

B. The H.E.S.S. experiment

The High Energy Stereoscopic System (H.E.S.S.) consists of four Imaging Atmospheric Cherenkov Telescopes (IACTs) [3]. It is designed to detect very high energy (VHE) γ -rays in the energy range from 100 GeV up to 100 TeV. H.E.S.S. detects Cherenkov light emitted from electromagnetic cascades of secondary particles resulting from the γ -ray/hadron primary interaction in the upper atmosphere. Cherenkov images of air showers are used to deduce the energy and direction of the primary particle. At the zenith, the energy threshold of the system is 100 GeV and for point sources, an energy resolution of 15% is achieved with stereoscopic measurements which determine the height of the maximum shower development. The angular resolution for individual γ -ray is better than 0.1° and the point source sensitivity for a 5σ detection reaches 1% of the flux of the Crab nebula in 25 hours [35]. The combination of these unequalled characteristics allows for detailed studies of high energy γ source morphology.

The future of H.E.S.S. is in an upgrade to the existing telescope array. H.E.S.S. phase II [36] consists of a very large single telescope located at the center of the H.E.S.S. I array, expected to start taking data as soon as end of 2008. The total mirror collection area is about 600 m^2 and the camera with a 3° field of view is made up of 2048 photomultiplier tubes. The pixel size of 0.07° will provide a better resolved shower image as compared to H.E.S.S. I. In the stand-alone operating mode, H.E.S.S. II will reach an energy threshold as low as 20 GeV.

C. Detection sensitivity of ground-based Cherenkov telescopes

The phase II of the ground-based Imaging Atmospheric Cherenkov Telescopes with its improved sensitivity at energies below 100 GeV and excellent angular resolution, may allow exploration of significant portions of the SUSY parameter space. Its sensitivity will depend strongly on the hadron background suppression procedures that will be developed at a few tens of GeV, unlike the space telescopes where the background is dominated by the diffuse photon emission. At present energies of H.E.S.S. I above 100 GeV threshold, the photon/hadron shower identification allows us to discover weak extended sources in a reasonable time of observation below 50 hours. One has to keep in mind that the phase II of H.E.S.S. will provide new results in the interesting astrophysical and/or new physics domains only if the steep hadron (proton, nuclei, etc) and cosmic electron spectra can be discarded. Forthcoming ACTs (such as the MAGIC II experiment [4] with two 17 m diameter telescopes) will investigate energies below 100 GeV. However, such ACTs are not expected to lower their energy thresholds as much as H.E.S.S. II will do, since these thresholds scale roughly linearly with the mirrors' size.

The following observation conditions of a given source will determine the effective sensitivity to the SUSY signal:

- the elevation angle as seen by H.E.S.S. on the horizon will have strong impact on the energy threshold, the hadron background suppression and energy resolution;
- the number of active telescopes, the zenith angle corresponding to a given source observation and its angular offset with respect to the center of the camera, will determine the acceptance values as a function of energy;
- the source spatial profile and weakness of the signal will condition the accepted number of γ and the power of the background suppression.

The optimal source observation conditions are currently fulfilled in H.E.S.S. experiment by the Galactic Center and Dwarf Spheroidal Galaxy observations.

Typical uncertainties on the integrated flux measured with H.E.S.S. are of the order of 20% which account mainly for systematics due to different signal extraction methods. The main contribution to these systematic effects come from the uncertainties on the hadron background suppression factors, strongly varying with the studied energy domain. As far as the low energy part of the spectrum is concerned, the data to come from H.E.S.S. phase II will allow us to explore the 20 GeV energy range for which there is no prior experience. The values quoted here are provided by Monte Carlo studies relying on the extrapolation from higher energies. The impact of the energy resolution on the energy threshold determination may be considered as negligible. The foreseen experimental uncertainty is still much less than the astrophysical uncertainties (see also section 4).

D. Sensitivity calculation

In the case of Cherenkov telescopes where the signal is extracted by ON-OFF subtraction, the significance S is given by [37]

$$S = \frac{N_\gamma}{\sqrt{2N_{bck}}} \quad (4)$$

where N_γ is the number of detected photons from DM annihilations, and N_{bck} the number of background photons.

For each annihilation of neutralino pairs, the differential continuum photon spectrum dN_γ/dE_γ expected from SUSY signals can be approximated [38, 40]:

$$\frac{dN_\gamma}{dE_\gamma} = \frac{1}{m_\chi} \left[\frac{10}{3} + \frac{5}{12} \left(\frac{E_\gamma}{m_\chi} \right)^{-3/2} - \frac{5}{4} \left(\frac{E_\gamma}{m_\chi} \right)^{1/2} - \frac{5}{2} \left(\frac{E_\gamma}{m_\chi} \right)^{-1/2} \right] \quad (5)$$

This leading-log approximation is obtained from a quark fragmentation model for the total hadron spectrum using the Hill spectrum. For more details, see [38]. On the other hand, the number of continuum photons above the energy threshold E_{th} collected by the telescope array can be expressed in terms of:

$$N_\gamma(E_\gamma > E_{th}) = T_{obs} \int_{E_{th}}^{\infty} A_{eff}(E_\gamma) \frac{d\Phi_\gamma}{dE_\gamma} dE_\gamma \quad (6)$$

where $A_{eff}(E_\gamma)$ corresponds to the effective area of the H.E.S.S. instrument for given energy, zenith angle, etc., T_{obs} the observation time, and $d\Phi_\gamma/dE_\gamma$ the differential γ -ray flux from DM particle annihilations calculated with the formula given in Eq. (2). Using Eq. (5) and Eq. (6) and inserting the expression of $d\Phi_\gamma/dE_\gamma$, after integration one can compute the minimum detectable annihilation rate $\langle\sigma v\rangle_{min}$:

$$\langle\sigma v\rangle_{min} = \frac{4\pi}{\bar{J}(\Delta\Omega) \Delta\Omega} \frac{S m_\chi^2 \sqrt{2 N_{bck}}}{\int_{E_{th}}^{\infty} A_{eff}(E_\gamma) \frac{dN_\gamma}{dE_\gamma} dE_\gamma} \quad (7)$$

For the signal under consideration, the major sources of background are protons, nuclei and electrons. Since the nuclei background is subdominant compared to others, this background will be neglected in what follows.

In the case of the hadronic background, the computation of the number of background events to be detected is derived using the following expression [20]:

$$\frac{d\Phi_{had}}{d\Omega}(E > E_{th}) = 6.1 \times 10^{-3} \epsilon_{had} \left(\frac{E_{th}}{1 \text{ GeV}} \right)^{-1.7} \quad (8)$$

[$\text{cm}^{-2}\text{s}^{-1}\text{sr}^{-1}$]

where ϵ_{had} represents the expected hadronic rejection which is in the case of H.E.S.S. II of the order of 80%. The contribution from cosmic ray electrons that initiate showers, which is not distinguishable from γ -rays, is [20]:

$$\frac{d\Phi_{e^-}}{d\Omega}(E > E_{th}) = 3.0 \times 10^{-2} \left(\frac{E_{th}}{1 \text{ GeV}} \right)^{-2.3} \quad (9)$$

[$\text{cm}^{-2}\text{s}^{-1}\text{sr}^{-1}$]

IV. CONSTRAINTS FROM H.E.S.S. II ON GAMMA-RAY FLUXES

In the framework described in Sec. II, the SUSY spectrum has been computed for various configurations in the Focus Point region. The scanned parameter region is defined in Table I. For each set of parameters, the integrated γ -ray flux has been derived using Eq. (2) integrated above the energy threshold. We assume as a benchmark halo shape a NFW profile which corresponds to a standard distribution for dark matter. A second less optimistic halo parametrization, presenting a core profile

TABLE I: The case study parameter region in the Focus point regime. The top mass m_t is set to 175 GeV (see text for discussions on sensitivity to m_t .)

Parameter	Minimum	Maximum
m_0 (GeV)	2200	5200
$m_{1/2}$ (GeV)	150	750
	$sign(\mu) = +1$	
	$\tan\beta = 10$	
	$A_0 = 0$	

with asymptotically flat velocity dispersion curve, has been also considered. Table II reports the value of the astrophysical quantity \bar{J} defined in Eq. (3) for the Galactic Center, in the case of the two aforementioned halo profiles for comparison. The resulting range of variation of \bar{J} allows us to estimate the magnitude of the astrophysical uncertainties affecting the determination of the γ -ray flux from neutralino annihilation. Fig. 1 presents the 5σ exclusion limit of H.E.S.S. II for the annihilation cross-section using a given acceptance parametrization $A_{eff}(E_\gamma)$, calculated for a generic Galactic Center source with a NFW and a cored DM profile respectively. Assuming an observation time of 50 hours and a 20 GeV energy threshold, a sensitivity as low as $\mathcal{O}(10^{-26}) \text{ cm}^3\text{s}^{-1}$ for the velocity-weighted annihilation cross-section can be achieved in case of a NFW profile. The SUSY models from Table I are also shown. In the scanned region, neutralino masses range from 50 GeV up to 300 GeV and velocity-weighted cross-sections from 10^{-29} up to $\sim 10^{-25} \text{ cm}^3\text{s}^{-1}$. The lowest neutralino masses as well as

TABLE II: Values of $\bar{J}(\Delta\Omega)$ for the Galactic Center with a NFW and cored profiles respectively [33] for the solid angle $\Delta\Omega = 2 \times 10^{-5} \text{ sr}$.

Profile	$\bar{J} (10^{23} \text{ GeV}^2 \text{ cm}^{-5})$
NFW	270
Core	0.7

annihilation cross-sections are reached through the monoenergetic lines resulting from loop-induced processes such as $\chi\chi \rightarrow \gamma\gamma$, $\chi\chi \rightarrow \gamma Z$ and $\chi\chi \rightarrow \gamma h$. A large fraction of the models obtained in the scan are within the reach of H.E.S.S. II in the case of a NFW halo profile. This opens the possibility to test a fraction of these models which satisfy constraints on the CDM relic density coming from the Wilkinson Microwave Anisotropy Probe (WMAP) [39]. As for comparison, in the case of the cored halo profile, the H.E.S.S. II sensitivity reaches $\sim 10^{-23} \text{ cm}^3\text{s}^{-1}$ and will not be able to constrain this parameter space region.

The same model set, defined in Table I, is shown in the left-hand side panel of Fig. 3 in the $(m_0 - m_{1/2})$ plane for a NFW profile. The higgsino content of the lightest neutralino χ implies large annihilation via W^+W^- , ZZ gauge bosons and substantial amount of γ -rays in the final state. For illustration, a typical value of m_0 as high as 3000 GeV is required to obtain a satisfactory value of the neutralino relic density for $m_t = 175$ GeV and $m_{1/2} = 300$ GeV. Furthermore, as the annihilation channels leading to γ -rays control also the thermal relic density, we observe a strong (anti)correlation between the latter and the γ -ray flux ϕ_γ . As can be seen from left panel of Fig. 3, ϕ_γ spans 5 orders of magnitude, while the relic density can vary rapidly over 3 orders of magnitude in the considered parameter space region as shown in Fig. 2.

Only a narrow region can accommodate the WMAP constraints on the CDM relic density. In order to account for these constraints, we highlight the models yielding a neutralino relic density lying in the range $0.067 \leq \Omega_\chi h^2 \leq 0.156$ (corresponding roughly to 5 standard deviations). The FP region is extremely sensitive to the value of the top mass m_t . Indeed, for large m_0 values the steep running of the m_{Hu} Higgs doublet mass term translates into a high sensitivity of the μ parameter to m_t through the requirement of radiative electroweak

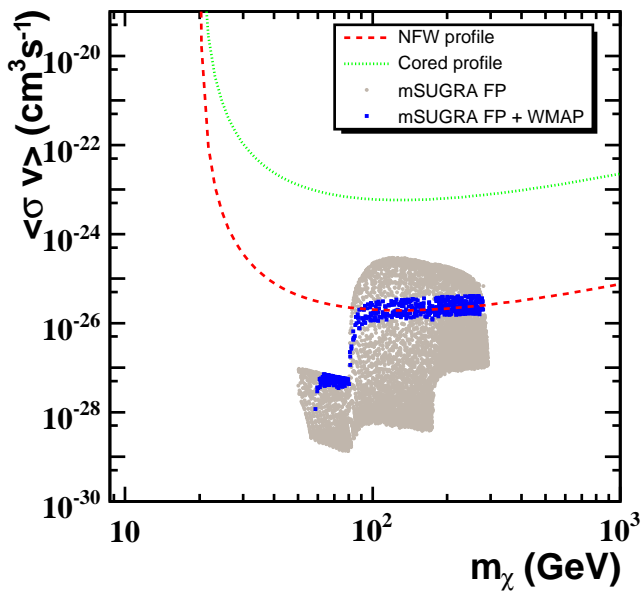


FIG. 1: 5σ exclusion limits for H.E.S.S. II on the velocity-weighted cross-section $\langle\sigma v\rangle$ as a function of the neutralino mass m_χ for the Galactic Center with a NFW profile (dashed red line). Also indicated is the case of a cored profile (dotted green line). The energy threshold is 20 GeV and the observation time is 50 hours. mSUGRA models (grey points) from the FP scanned region defined in Table I are presented as well as those satisfying WMAP constraints on the CDM relic density (blue points).

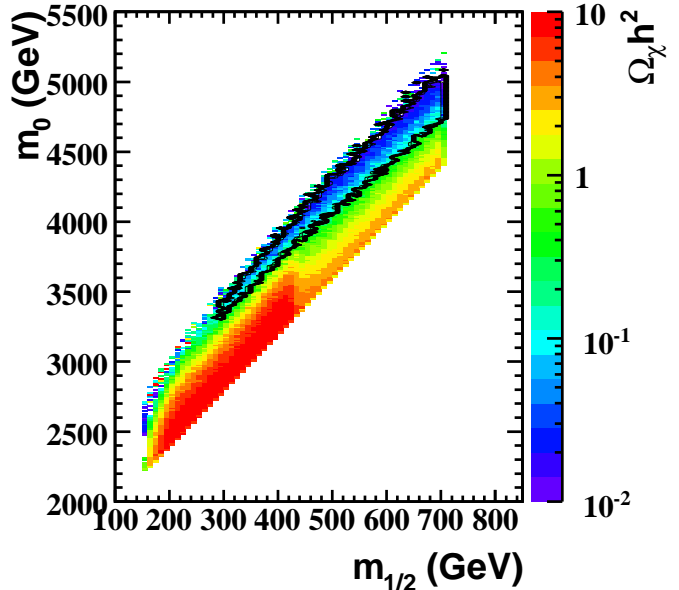


FIG. 2: Neutralino relic density, $\Omega_\chi h^2$, in the $(m_0, m_{1/2})$ plane for the FP region defined in Table I with $A_0 = 0$, $\tan\beta = 10$, $\text{sign}(\mu) = +1$ and $m_t = 175$ GeV. Overlaid is the H.E.S.S. II sensitivity for a 5σ detection in 50 hours (black contours).

symmetry breaking. As already mentioned in section 2, one can then obtain substantially different sparticle spectra when using different RGE codes [41]. It is well known that the above-mentioned strong sensitivity can lead to dramatically different $\Omega_\chi h^2$ values for a fixed choice of the mSUGRA input parameters $m_0, m_{1/2}$, etc. Thus using different codes can possibly require slight readjustment of the input parameter values to retrieve the appropriate WMAP allowed region. Nevertheless once a scan is performed over a reasonably large domain in the $(m_0, m_{1/2})$ plane, the effect of using different codes is simply to “shift around” a bit the different contours for the WMAP allowed ranges, eventually modifying somewhat their shapes, which has been checked to some extent in the present study using the code SuSpect [18]. Thus the discrepancies in the sparticle spectrum in the focus region, as obtained from the different publically available codes, should not affect appreciably our main results, provided of course that the same code is used consistently for the whole study.[59] However, we will occasionally present the output of two versions of ISAJET, 7.69 and 7.71, in order to better illustrate the range of reliability of the predicted observables.

The phenomenology of the FP region differs from the so-called bulk and co-annihilation regions due to the large masses of the sfermions. The scalar sector, including the CP even/odd and charged Higgs, lies in the few TeV range except for the lightest Higgs boson. In performing the scanning of SUGRA parameters, we have checked that a number of present experimental and theoretical

constraints are fulfilled. Apart from the direct lower limits on the sparticle masses obtained at LEP or Tevatron [44] which are obviously fulfilled in the range of parameters we consider here, there are potentially some constraints from virtual supersymmetric contributions to low energy observables. The leading $\tilde{\chi}^{\pm}\tilde{t}$ and tH^{\pm} loop corrections to the branching ratio for radiative b decays, which can give in principle interesting constraints on supersymmetric models, are completely negligible in the present case due to the decoupling effects of the very heavy sfermion and charged Higgs masses. Similarly, supersymmetric contributions [45] to $a_{\mu} \equiv (g_{\mu} - 2)/2$, which would be typically enhanced for large values of the combination $\mu \times \tan\beta$ through charginos/sneutrinos (and more moderately neutralinos/smuons) one-loop corrections, are suppressed in our case due to the very large sfermion masses and moderate values of $\tan\beta$. In particular this focus point region would be consistent with the comparison between the measurements [46] and the standard model theoretical predictions [47] for a_{μ} , if the hadronic τ -decay data (rather than the $e^{+}e^{-}$ annihilation into hadrons) are used in the determination of the leading hadronic contribution [48].

The left panel of Fig. 4 shows the range of gluino masses, $m_{\tilde{g}}$, as a function of the two lightest neutralino mass difference, $m_{\chi_2^0} - m_{\chi_1^0}$, which is a key observable for ATLAS (see section 5), and the corresponding γ -ray flux. The latter observable is indirectly sensitive to the neutralino mass difference and somewhat in a model dependent way. In our mSUGRA constrained scenario, and given the LSP mass range and large m_0 values considered here, the ZZ and $W^{+}W^{-}$ annihilation channels are open and become actually dominant as compared to the fermion pair ($f\bar{f}$) final state channels. This is a combined effect of, on one hand the suppression of $f\bar{f}$ final states due to t -channel exchange of very heavy sfermions, and on the other hand a substantial higgsino component of the LSP enhancing its coupling to Z 's and W 's. A larger $m_{\chi_2^0} - m_{\chi_1^0}$ corresponds to heavier neutralinos (resp. charginos) which are exchanged in the t -channel, and thus reduces the ZZ (resp. $W^{+}W^{-}$) final states, implying an overall reduction of the γ -ray fluxes. The sensitivity of H.E.S.S. II is displayed as solid black contour. Models satisfying WMAP constraints on $\Omega_{\chi}h^2$ are also highlighted as dashed purple contours. Gluino masses lying in the range 800-1800 GeV are within the reach of H.E.S.S. II sensitivity for neutralino mass differences up to 80 GeV. Given the WMAP constraints, a significant fraction of cosmologically interesting SUSY models will be tested with H.E.S.S. II.

V. LHC MEASUREMENTS

The scan described in the previous sections was performed over a region of mSUGRA space for which $m_{\tilde{g}} \leq 1800$ GeV. Various studies are available in the literature [50, 51, 52, 53] which demonstrate that for an in-

tegrated luminosity of $\sim 100 \text{ fb}^{-1}$ inclusive searches for events including multiple jets and/or leptons and missing transverse energy would allow the discovery at the LHC of gluino production up to masses of ~ 1800 GeV, thus covering most of the investigated region.

Beyond the mere discovery of a signal, the LHC should be able to perform measurements of the SUSY spectrum which would allow the experiments to put constraints on the predicted relic density [10, 54, 55]. One point in the region addressed here was studied in detail in [49], and the possible ways of extracting a parameter measurement were investigated. It turned out that the cleanest signal for parameter measurements would be the study of the three-body decay

$$\chi_{2(3)}^0 \rightarrow \ell^{+}\ell^{-}\chi_1^0 \quad (10)$$

where the $\chi_{2(3)}^0$ would be produced in the decay $\tilde{g} \rightarrow qq\chi_{2(3)}^0$. Alternatively the same signal could be searched for through the direct production of neutralinos in association with charginos in proton-proton interactions.

This chain would give a clean final state signature [50] with two opposite-sign same-flavour leptons. The kinematics of the three-body decay imply that the invariant mass of any two particles in the decay must be smaller than the difference between the mass of the mother particle and the mass of the remaining particle. Therefore, from the observation of one (or more) kinematic end-points in the invariant mass distribution of the two leptons from the decay given in Eq. (10) the mass difference $m_{\chi_i^0} - m_{\chi_1^0}$ can be measured. The error on this measurement has a systematic component, arising from lepton selection cuts, and a statistical component which will scale both with the value of the mass difference and with the number of events observed. This latter component will vary over the SUSY parameter space due to variations in the mass spectrum and in the total SUSY production cross-section. For the model studied in [49], a precision of order 1% is obtained, which reflects the excellent measurement capabilities of the LHC experiments for leptons.

We have investigated the LHC reach for this measurement for the region of mSUGRA space defined in section 4, by calculating the number of events expected at the LHC for the decay given in Eq. (10) for an integrated luminosity of 100 fb^{-1} . The number of events shown are independent of the detector assumptions. For the quoted selection efficiencies we refer to an ATLAS analysis in parametrised simulation. The results are valid for the generic performance of an LHC detector and are expected to be equivalent for CMS. We used ISAJET 7.71 [56] for the calculation of spectra and branching fractions and Prospino [57] for the NLO cross-section for gluino production. The results are shown in the right-hand side panel of Fig. 3 in the $(m_0 - m_{1/2})$ plane before selection efficiency cuts. The sharp cut on the right-hand side is due to the fact that we do not consider models for which $m_{\chi_2^0} - m_{\chi_1^0} > 85$ GeV, at which point the kinematic end

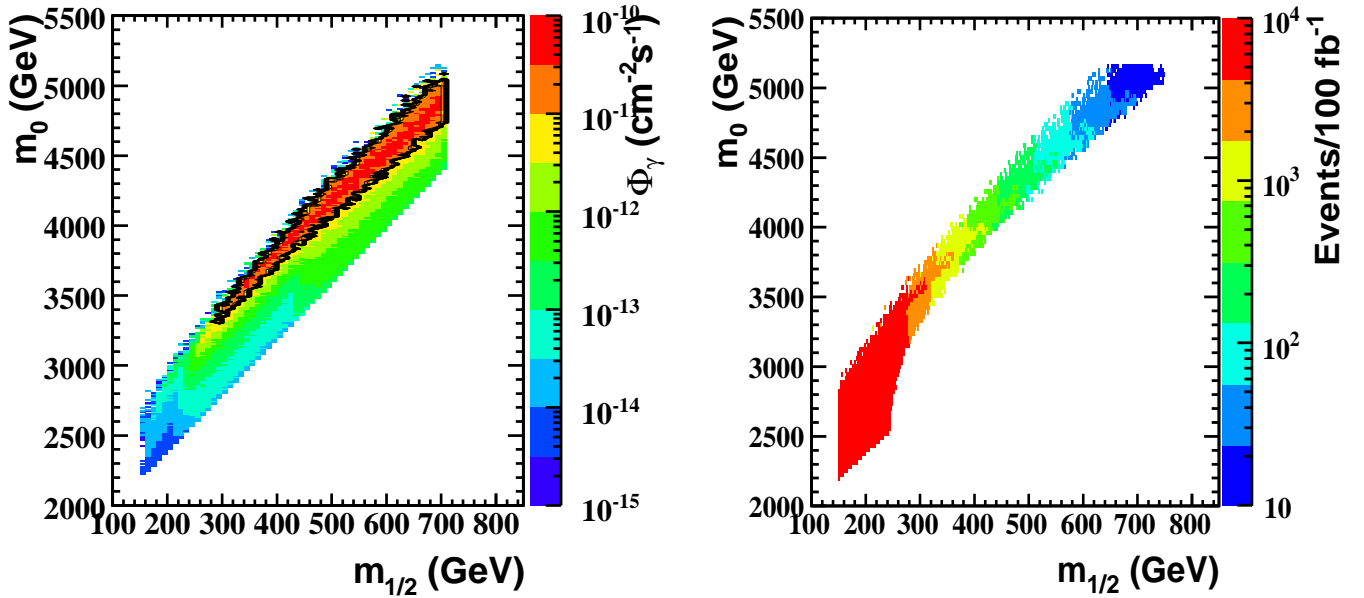


FIG. 3: Left: Integrated γ -ray flux above 20 GeV, Φ_γ , in the $(m_0, m_{1/2})$ plane for the FP region defined in Table I with $A_0 = 0$, $\tan\beta = 10$, $\text{sign}(\mu) = +1$ and $m_t = 175$ GeV. Overlaid is the H.E.S.S. II sensitivity for a 5σ detection in 50 hours (black contours). Right: Expected number of signal events before selection efficiency cuts for the leptonic 3-body decay of neutralinos (see Eq. (10)) at the LHC for an integrated luminosity of 100 fb^{-1} in the $(m_0 - m_{1/2})$ plane.

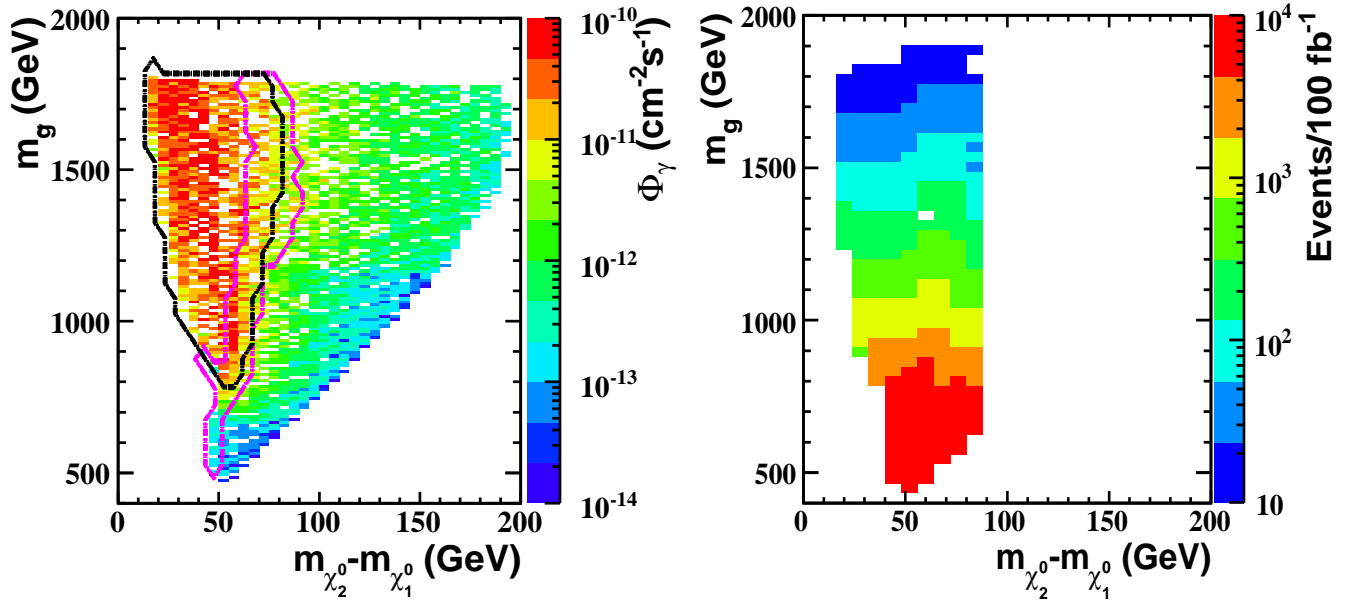


FIG. 4: Left: Integrated γ -ray flux above 20 GeV in the FP region defined in Table I in the plane of the gluino mass, $m_{\tilde{g}}$, as a function of the mass difference of the two lightest neutralinos $m_{\chi_2^0} - m_{\chi_1^0}$. Overlaid are the H.E.S.S.-II sensitivity (solid black contour) and the 5σ allowed range from WMAP $\Omega_{CDM} h^2$ measurements (dashed purple contour). Right: Expected number of signal events before selection efficiency cuts for the leptonic 3-body decay of neutralinos (see Eq. (10)) at the LHC for 100 fb^{-1} in the $(m_{\chi_2^0} - m_{\chi_1^0}, m_{\tilde{g}})$ plane.

point in the two-lepton invariant mass distribution starts to be masked by the Z peak that arises from the decay in two leptons. When the decay $\chi_2^0 \rightarrow Z\chi_1^0$ becomes kinematically accessible (i.e. when the neutralino mass difference exceeds the Z mass), the previous kinematic signature resulting from a three-body decay is lost, and the two body process that occurs instead does not allow us to make an unambiguous and model independent measurement of the neutralino mass difference. This two body process will dominate up to the point where a neutralino decay channel featuring a light higgs h , $\chi_2^0 \rightarrow h\chi_1^0$, becomes open. The higgs decays mostly into $b\bar{b}$ pairs, and the extraction of the $h \rightarrow b\bar{b}$ peak above the large combinatorial of b jets from gluino decays is very challenging. For the three-body decay of the neutralinos to leptons, in the analysis of [49] an efficiency of $\sim 25\%$ is achieved for the signal, the SUSY background is ~ 0.6 times the signal, and a SM background of ~ 250 events is expected for 100 fb^{-1} . The SM background is dominated by $t\bar{t}$ production. This background, as well as the SUSY backgrounds, can be easily evaluated from the data themselves. In fact the two leptons from the three-body decays of the neutralino, being from the decay of a virtual Z, must have the same flavour and opposite sign. The two isolated leptons from $t\bar{t}$ are produced from the decays of two W and can therefore have any flavour combination. It is therefore easy to statistically subtract the background by subtracting the invariant mass distribution of $e^\pm\mu^\mp$ pairs from the sum of the distributions for $e^\pm e^\mp$ and $\mu^\pm\mu^\mp$ pairs. Equivalent considerations are valid for the SUSY backgrounds, where the flavours of the two leptons are uncorrelated. Assuming that the efficiency of the analysis cuts and ratio between signal and SUSY background do not vary dramatically in the investigated region, a signal of ~ 350 events would be needed for the observation at 5σ level for an integrated luminosity of 100 fb^{-1} . The number of signal events is essentially determined by the gluino mass, as is clear in the right panel of Fig. 4, where the number of signal events is given on the $(m_{\chi_2^0} - m_{\chi_1^0}, m_{\tilde{g}})$ plane. The opposite sign - same flavour two-lepton signal should therefore be observable for $m_{\tilde{g}} \leq 1300 \text{ GeV}$.

VI. DISCUSSION OF THE COMPLEMENTARITY

We discuss here the complementarity of the indirect detection with the phase II of H.E.S.S. and the ATLAS searches at LHC in the focus point region.

The potentialities of the two experiments in the FP region can be readily compared through the integrated γ -ray flux and the expected number of signal events for Next-to-LSP 3-body leptonic decays, in the $(m_0, m_{1/2})$ plane, displayed respectively in the left and right panels of Fig. 3. The left-hand side plot of Fig. 3 shows the H.E.S.S. γ -ray flux contours for a 5σ detection. The H.E.S.S. γ -ray integrated flux sensitivity which is at the

level of $\sim 10^{-12} \text{ cm}^{-2}\text{s}^{-1}$, allows us to test SUSY models characterized by universal scalar soft mass parameters above 3300 GeV and gaugino soft mass parameters above 280 GeV. From the number of signal events for 100 fb^{-1} in the 3-body leptonic decay shown in the right panel of Fig. 3, the ATLAS sensitivity will allow us to investigate m_0 lower than 4200 GeV and $m_{1/2}$ as high as 550 GeV. Thus the combination of the sensitivity of each experiment allows us to cover the overall region. This point highlights the complementarity between the indirect detection of dark matter and the SUSY searches at LHC. Moreover, an overlap is obtained in a small region characterized by scalar soft masses in the 3300-4200 GeV range and gaugino soft masses between 280 and 550 GeV. In case of a signal discovery consistent with this region, complementary cross-checks between the two experiments would lead to further constraints on the allowed parameter space in the $(m_0, m_{1/2})$ plane.

For further illustration, we have chosen in Fig. 4 a given point in the parameter space:

$$m_0 = 3350 \text{ GeV}, m_{1/2} = 300 \text{ GeV}, A_0 = 0 \text{ GeV}, \\ \mu > 0, \tan \beta = 10 \quad (11)$$

This point, with the top mass set to 175 GeV and the mass spectrum computed with ISAJET, is close to the point (sometimes dubbed SU(2)) which has been chosen by the ATLAS experiment for a detailed study [49]. For each quantity reported in Table III, two values are given corresponding to the output spectra of ISAJET7.69 and ISAJET7.71. This allows to give an estimate for the theoretical uncertainties. As can be seen from Fig. 4 and Table III, this particular point, which is within the reach of ATLAS, is also within the reach of H.E.S.S. II provided a typical 50 hours observation time of a Galactic Center type source.

As explained in section V, a key parameter in the ATLAS sensitivity is the gluino mass. The sensitivity curves of each experiment allow to constrain different regions in the plane of the gluino mass versus the mass difference of the two lightest neutralinos as shown in Fig. 4. As can be seen, one anticipates lower flux values for larger neutralino mass differences. Given an astrophysical model for the source (see section 4), H.E.S.S. II would thus put lower limits on the neutralino mass differences which can be further refined with some knowledge of the gluino mass. Moreover, given the sensitivity zone of H.E.S.S. II, one finds that a larger gluino mass would allow the exploration of a larger fraction of the parameter space. In contrast, and as illustrated in from Fig. 4, ATLAS will have larger sensitivities for lighter gluinos. In any case, and irrespective of the gluino mass, the extraction of information from ATLAS measurements becomes problematic for a neutralino mass difference exceeding 85 GeV. Finally, comparing the two considered observables in the panels of Fig. 4 one notes a reversed sensitivity to the mass parameters: ATLAS would provide a strong constraint on the gluino mass whereas the indirect detection is more sensitive to the neutralino mass differences. Or-

TABLE III: Values of the neutralino relic density $\Omega_\chi h^2$, the γ -ray flux Φ_γ , the number of events per 100 fb $^{-1}$ after selection efficiency cuts for NLSP 3-body leptonic decays, the mass difference of the two lightest neutralinos and the gluino mass, for the SUSY point defined in Eq. (11). The two quoted values for each observable correspond respectively to the output of ISAJET 7.69 and 7.71 (see text for details).

Relic density $\Omega_\chi h^2$		γ -ray flux Φ_γ (cm $^{-2}$ s $^{-1}$)		Events per 100 fb $^{-1}$		$m_{\chi_2^0} - m_{\chi_1^0}$ (GeV)		$m_{\tilde{g}}$ (GeV)
0.06	0.16	6.6×10^{-12}	2.3×10^{-12}	855	468	55	88	852

thogonal constraints can thus be obtained by indirect detection and collider searches, and their possible combination would reduce significantly the allowed parameter space.

VII. CONCLUSION AND PERSPECTIVES

In this paper we have examined the complementarity of two approaches to unravel signatures of dark matter particles in the case where the latter are neutralino LSPs in the Focus Point region of the mSUGRA scenario. Searches at colliders in this region which is difficult to investigate as compared to the so-called bulk region, will benefit from complementary input from indirect searches through γ -rays[60]. In the present study we used the most realistic simulations for both ATLAS and H.E.S.S. II for which we considered the Galactic Center as a benchmark astrophysical DM source. We found that the two experiments will typically explore two different regions of the studied parameter space with some possible overlap, allowing in principle complementary analyses. We illustrated these features in terms of the universal soft parameters as well as in terms of the physical masses, the first corresponding to a top-down model-dependent approach while the second illustrates the more challenging model-independent one. For instance, in the scanned range of neutralino LSP masses from 50 to 300 GeV, ATLAS will be sensitive to gluinos lighter than 1300 GeV whereas H.E.S.S. II, with a flux sensitivity of the order of

10^{-12} cm $^{-2}$ s $^{-1}$, will be able to cover all the region above 1 TeV. Furthermore, the mass difference of the two lightest neutralinos which is a key observable for ATLAS, is interestingly found to be a sensitive parameter for the γ -ray fluxes that H.E.S.S. II can observe or constrain.

More generally, in the very near future, H.E.S.S. II and LHC will be two major experiments allowing us to probe the supersymmetric hypothesis for dark matter with an, up to now, unequalled capability. Neutralino masses in the yet uncovered 100 GeV range will be accessible to H.E.S.S. II thus filling the energy gap between the current H.E.S.S. I and the GLAST satellite experiment to be launched in Spring 2008. Finally, if SUSY signals are discovered at the LHC, the cross-sections, branching ratios and masses of the new particles determined with a few fb $^{-1}$ luminosity, would provide valuable search windows both for direct and indirect supersymmetric dark matter detection. Of course, substantial systematic uncertainties arise on the astrophysical parameters in indirect searches, which can be reduced through an improved knowledge of the halo profiles of the observed sources. Direct detection also suffers from systematic effects related to astrophysical and nuclear parameter uncertainties which affect the constraints on the nucleon-WIMP cross-sections. The more model-independent measurements of the SUSY parameters will require data samples collected with hundreds of fb $^{-1}$ luminosity at the LHC, as well as independent input from indirect (or direct) dark matter searches as illustrated in this paper.

-
- [1] H. Goldberg, Phys. Rev. Lett. 50 (1983) 1419; J. Ellis *al.*, Nucl. Phys. B **238** (1984) 453.
 - [2] for reviews, see for instance G. Jungman, M. Kamionkowski and K. Griest, Phys. Rep. **267** (1996) 195, and G. Bertone, D. Hooper and J. Silk, Phys. Rep. **405** (2005) 279.
 - [3] <http://www.mpi-hd.mpg.de/hfm/HESS/HESS.html>
 - [4] <http://hegral.mppmu.mpg.de/MAGICWeb/>
 - [5] <http://veritas.sao.arizona.edu/index.html>
 - [6] <http://ams.cern.ch/>
 - [7] <http://www-glast-stanford.edu/>
 - [8] <http://wizard.roma2.infn.it/pamela/>
 - [9] LHC/LC Study Group: G. Weiglein *et al.*, Phys. Rep. **426** (2006) 47.
 - [10] E. A. Baltz, M. Battaglia, M. E. Peskin and T. Wizansky, Phys. Rev. D **74** (2006) 103521.
 - [11] D. Hooper and A. M. Taylor, JCAP **0703** (2007) 017.
 - [12] V. Barger, W. Y. Keung, G. Shaughnessy and A. Tregre, Phys. Rev. D **76** (2007) 095008.
 - [13] J. Feng, K. Matchev and T. Moroi, Phys. Rev. Lett. **84** (2000) 2322 and Phys. Rev. D **61** (2000) 075005.
 - [14] J. Feng, K. Matchev and F. Wilczek Phys. Lett. B **482** (2000) 388 and Phys. Rev. D **63** (2001) 045024.
 - [15] H. Baer *et al.*, JHEP **0510** (2005) 020 and references therein.
 - [16] H. Baer, T. Krupovnickas and X. Tata, JHEP **0307** (2003) 020; B. C. Allanach, S. Kraml and W. Porod, JHEP **0303** (2003) 016; G. Belanger, S. Kraml and

- A. Pukhov, Phys. Rev. D **72** (2005) 015003.
- [17] Isajet v7.72, H. Baer *et al.*, arXiv:hep-ph/0312045.
- [18] SuSpect 2.34, A. Djouadi, J.-L. Kneur and G. Moultaka, Comput. Phys. Commun. **176** (2007) 426.
- [19] P. Gondolo *et al.*, JCAP **0407** (2004) 008.
- [20] L. Bergström, P. Ullio and J. Buckley, Astropart. Phys. **9** (1998) 137.
- [21] E. A. Baltz, C. Briot, P. Salati, R. Taillet and J. Silk, Phys. Rev. D **61** (1999) 023514.
- [22] N. Fornengo *et al.*, Phys. Rev. D **70** (2004) 103529.
- [23] A. Tasitsiomi *et al.*, Astropart. Phys. **21** (2004) 637.
- [24] N. W. Evans, Mon. Not. Roy. Astron. Soc. **260** (1998) 190.
- [25] J. Navarro, C. Frenk and S. White, Astrophys. J. **462** (1996) 563.
- [26] B. Moore *et al.*, Phys. Rev. D **64** (2001) 063508.
- [27] J. J. Binney and N. W. Evans, Mon. Not. Roy. Astron. Soc. **327** (2001) L27.
- [28] V. Debattista and J. A. Selwood, Astrophys. J. **493** (1998) L5.
- [29] J. J. Binney, O. E. Gerhard and J. Silk, Mon. Not. Roy. Astron. Soc. **321** (2001) 471.
- [30] P. McMillan and W. Dehnen, Mon. Not. Roy. Astron. Soc. **363** (2005) 1205.
- [31] F. A. Aharonian *et al.* (H.E.S.S. Collaboration), Astronomy and Astrophysics **425** (2004) L13.
- [32] F. A. Aharonian *et al.* (H.E.S.S. Collaboration), Nature **439** (2006) 695.
- [33] N. W. Evans, F. Ferrer and S. Sarkar, Phys. Rev. D **69** (2004) 123501.
- [34] F. A. Aharonian *et al.* (H.E.S.S. Collaboration), Astropart. Phys. **29** (2008) 55.
- [35] F. A. Aharonian *et al.* (H.E.S.S. collaboration), Astronomy and Astrophysics **457** (2006) 899.
- [36] M. Punch (for the H.E.S.S. collaboration), Proc. of Cherenkov 2005, Towards a Network of Atmospheric Cherenkov Detectors VI, April 2005, Ecole Polytechnique, Palaiseau, France.
- [37] T. P. Li and Y. Q. Ma, Astrophys. J. **272** (1983) 317.
- [38] A. Tasitsiomi and A. V. Olinto, Phys. Rev. D **66** (2002) 083006.
- [39] <http://map.gsfc.nasa.gov/>
- [40] A. Jacholkowska *et al.*, Phys. Rev. D **74** (2006) 023518.
- [41] <http://cern.ch/kraml/comparison/> and the third reference in [16].
- [42] B. C. Allanach, Comput. Phys. Commun. **143** (2002) 305.
- [43] W. Porod, Comput. Phys. Commun. **153** (2003) 275.
- [44] Particle Data Group, J. of Phys. G **33** (2006) 1.
- [45] S. P. Martin and J. D. Wells, Phys. Rev. D **64** (2001) 035003; G. Degross and G. F. Giudice, Phys. Rev. D **58** (1998) 053007.
- [46] Muon $g - 2$ Collaboration, G.W. Bennett *et al.*, Phys. Rev. Lett. **89** (2002) 101804, Erratum-ibid. Phys. Rev. Lett. **89** (2002) 129903 and Phys. Rev. Lett. **92** (2004) 161802.
- [47] M. Davier *et al.*, Eur. Phys. J. **C31**, 503 (2003); K. Hagiwara, A. D. Martin, D. Nomura and T. Teubner, Phys. Rev. D **69** (2004) 093003.
- [48] See e.g. for a recent review M. Passera, talk given at the Tau06 Workshop, Pisa, Sept. 2006, hep-ph/0702027.
- [49] U. De Sanctis *et al.*, Eur. Phys. J. C **52** (2007) 743.
- [50] ATLAS Collaboration, *ATLAS detector and physics performance Technical Design Report*, CERN/LHCC 99-14/15 (1999); <http://atlas.web.cern.ch/Atlas/GROUPS/PHYSICS/TDR/access.htm>
- [51] CMS Collaboration *CMS physics : Technical Design Report v.2 : Physics performance* CERN-LHCC-2006-021 (2006); <http://cdsweb.cern.ch/search.py?recid=942733>.
- [52] D. R. Tovey, Eur. Phys. J. C **4** (2002) N4.
- [53] H. Baer *et al.*, JHEP **0306** (2003) 054.
- [54] G. Polesello and D. R. Tovey, JHEP **0405** (2004) 071.
- [55] M. M. Nojiri, G. Polesello and D. R. Tovey, JHEP **0603** (2006) 063.
- [56] H. Baer *et al.*, arXiv:hep-ph/0312045.
- [57] W. Beenakker *et al.*, Nucl. Phys. B **492** (1997) 51.
- [58] the acronym mSUGRA is used everywhere in this paper in a loose sense, that is without assuming a GUT scale relation between the soft parameters A_0 and B_0 that would result from a flat Kähler metric.
- [59] More precisely the most important differences occur in fact between Isajet 7.69 on one side and Suspect/SoftSuSy [42]/Spheno [43] on the other for the determination of the μ parameter, while the differences among the latter three codes appear to be generally much milder [41]. It should be noted however that the discrepancies in the LSP neutralino mass remain moderate even though in the focus point region its higgsino component is not negligible, since the neutralino N_1 component remains essentially determined by the $U(1)_Y$ gaugino soft mass term M_1 in this region, so that its mass is not very sensitive to μ .
- [60] We note that searches in the bulk region are easier due to the fact that the lower value of m_0 ensures that squarks and sleptons will be visible at the LHC. The greater range of visible sparticles will provide a greater knowledge of the sparticle mass spectrum.